A Journal of
ChemPubSoc Europe

EurJIC
European Journal of Inorganic Chemistry

Accepted Article

Title: Synthesis, Electrochemistry and Optical Properties of Half-sandwich Ruthenium Complexes Bearing Triarylamine-Anthracenes

Authors: Eduard Kovalski, Marcus Korb, and Alexander Hildebrandt

To be cited as: *Eur. J. Inorg. Chem.* 10.1002/ejic.201701409

Link to VoR: http://dx.doi.org/10.1002/ejic.201701409

WILEY-VCH

10.1002/ejic.201701409

Synthesis, Electrochemistry and Optical Properties of Half-sandwich Ruthenium Complexes Bearing Triarylamine-Anthracenes

Eduard Kovalski,[a] Marcus Korb[a] and Alexander Hildebrandt*[a]

Abstract: The complex [CpRu^{II}(dppe)(taae)] (Cp = η^5-C_5H_5, dppe = 1,2-$(PPh_2)_2$-C_2H_4, taae = 10-ethynyl-*N*,*N*-di-*p*-tolylanthracen-9-amine) has been synthesized in a multistep reaction protocol including Sonogashira *C*,*C*- and Buchwald-Hartwig *C*,*N*- cross coupling reactions. Electrochemical and spectroscopic studies suggest a high degree of delocalization between the ruthenium and triarylamine termini through the anthracene bridge, forming a donor-π-acceptor (D-π-A) dye whose π-π* transitions exhibit charge transfer character in the monocationic oxidation state.

Introduction

More than 50% of the solar radiation reaching the Earth's surface lies within the near-infrared, hence considerable effort is presently devoted to developing photosensitizers with superior absorption properties in that energy range.[1–4] Cationic bis(triarylamine) systems usually display intense NIR absorptions arising from intervalence charge transfer (IVCT) in addition to the intensive π-π* transitions localized at the NAr_3^+ functionalities. Further oxidation to dications with two NAr_3^+ sites quenches the IVCT band.[5–7] The properties of these IVCT bands can be varied by the choice of substituents and a good stability of their radical cations once the *para* positions are blocked to avoid benzidine-type rearrangements.[8] Properties similar to the triarylamines can be achieved with ruthenium half-sandwich compounds, showing one usually reversible one-electron oxidation per ruthenium subunit at rather low formal potentials.[9,10] They exhibit a rich electrochemistry with a strong substituent dependence of the redox potentials. The combination of triarylamine and Ru-half-sandwich complexes leads to a donor-π-acceptor (D-π-A) dye whose π-π* transitions exhibit charge transfer character.[11] Herein, we describe the synthesis and (spectro-)electrochemical properties of a NIR-dye combining both triaryl and ruthenium units with anthracene as an extended π-bridging system.

Results and Discussion

9-Bromo-10-di(*p*-tolyl)aminoanthracene (**1**) is accessible by a three step synthetic procedure including the bromination of anthracene, subsequent Buchwald-Hartwig amination[12], and bromination of the resulting anthracenyl-amine in 10-position. The bromination of anthracene was performed following a modified reaction protocol[13] using a solution of NBS (*N*-bromosuccinimide) in tetrahydrofuran to give 9-bromo-anthracene in 84 % yield, which had to be separated from 9,10-dibromoanthracene by recrystallization from ethanol. 9-bromoanthracene was converted to di(*p*-tolyl)aminoanthracene by a palladium catalyzed Buchwald-Hartwig amination with di(*p*-tolyl)amine. The second bromination was achieved by the reaction of di(*p*-tolyl)aminoanthracene with NBS in glacial acetic acid, which gave a faster and cleaner reaction than the literature described methodologies (see supporting information).[14]

Bromoanthracene **1** was converted to acetylene **2** by applying a palladium catalyzed Sonogashira *C*,*C* cross-coupling reaction with trimethylsilylacetylene using $[PdCl_2(PPh_3)_2]$ as catalyst in the presence of CuI (see Scheme 1).[15,16] The trimethylsilyl protecting group of **2** was removed by the reaction with tetrabutylammonium fluoride to give anthracenyl-acetylene **3** in almost quantitative yield. In the final reaction step, the ruthenium was introduced by a chlorine-acetylene exchange reaction using [CpRu(dppe)Cl] (Cp = η^5-C_5H_5; dppe = 1,2-bis(diphenylphosphino)ethane) as precursor complex (see Scheme 1) forming compound **4**.

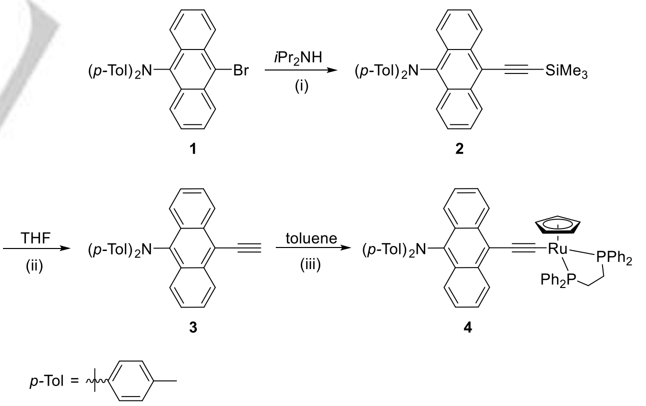

Scheme 1. Preparation of ruthenium complex **4** from bromoanthracene **1**. i) 82 °C, 17 h, 6 mol-% CuI, 1 mol-% $[PdCl_2(PPh_3)_2]$, 6 mol-% PPh_3.; ii) 66 °C, 15 h, 1.5 eq. tetrabutylammonium fluoride; iii) 111 °C, 17 h, 1.0 eq. CpRu(dppe)Cl, 9.8 eq. NaO*t*Bu.

Compounds **1** – **4** are stable towards air and moisture, in the solid state as well as in solution. They have been analyzed by NMR and IR spectroscopy as well as elemental analysis and HR-ESI-TOF- mass spectrometry. The molecular structures of **2** (CCDC 1588283) and **3** (CCDC 1588284) in the solid state could be determined by single crystal x-ray diffraction, however we were not able to obtain suitable single crystals of **4**. The electrochemical behavior of **2** and **4** have been characterized by cyclic and square wave voltammetry. In addition the electronic properties of **4**, 4^+ and 4^{2+} have been investigated by UV/Vis-NIR

---

[a] Technische Universität Chemnitz, Fakultät für Naturwissenschaften, Institut für Chemie, Anorganische Chemie
09107 Chemnitz, Germany
E-mail: alexander.hildebrandt@chemie.tu-chemnitz.de
https://www.tu-chemnitz.de/chemie/anorg/ah/ah.php

spectroelectrochemisty measurements. Furthermore, **3** and **4** were studied by fluorescence spectroscopy.

Conversion of **1** to **2** leads to the appearance of signals for the $SiMe_3$ group (0.45 ppm ^1H; 0.4 ppm $^{13}C\{^1H\}$) as well the resonances for the *C*,*C* triple bond carbon atoms at 107.1 and 101.7 ppm respectively. The deprotection of the acetylene from **2** to **3** can be monitored by the disappearance of the signals for $SiMe_3$ group and the observation of the ≡C-H proton signal at 4.05 ppm. Introduction of the Ru-half-sandwich moiety in compound **4** is accompanied with the observation of resonance signals for the Cp unit at 4.98 ppm in ^1H NMR as well as 83.1 ppm in $^{13}C\{^1H\}$ NMR and the dppe ligand (multiplets at 2.26–2.33 and 2.43–2.55 ppm in ^1H; 29.9 $^{13}C\{^1H\}$; 86.0 ppm $^{31}P\{^1H\}$). The deprotection and subsequent complexation of the acetylene unit for **2**, **3** and **4** can in addition be monitored during the reaction by IR spectroscopy. Whereby the $\tilde{\nu}_{C\equiv C}$ vibration is observed with a moderate strength at 2140 cm^{-1} in $SiMe_3$ protected **2** while in **3** this band is shifted to 2093 cm^{-1} and is only observed as a very weak absorption, however a strong band of the $\tilde{\nu}_{\equiv C-H}$ stretching can be observed at 3299 cm^{-1}. For compound **4** the $\tilde{\nu}_{C\equiv C}$ stretching vibration is found at 2043 cm^{-1}.

Suitable single crystals for X-ray diffraction of **2** and **3** were obtained by controlled evaporation of saturated solutions of the respective compounds in hexane. Both compounds crystallize in a monoclinic space group (**2**: $P2_1/c$; **3**: $P2_1/n$). The molecular structures of compounds **2** and **3** in the solid state are depicted in Figure 1. As common for anthracenyl units the peripherical benzene units are distorted from the ideal hexagon geometry by shortening the C8–C9, C10–C11, C15–C16 and C17–C18 bonds for compound **2** to approx. 1.36 Å while the C9–C10, C7–C12, C19–C14 and C16–C17 bonds are approx. 1.42 Å in length. The same pattern is observed for compound **3**. The anthracene rings themselves are not perfectly planar. The outer rings of the anthracene are titled with respect to a mean plane of the middle ring by 3.5(4) and 1.8(4)° (**2**) or 3.00(12) and 3.51(12) (**3**), respectively. The triaryl amino unit is twisted with respect to the anthracenyl units by 66.51(19)° (**2**) and 69.91(7)° (**3**), while the tolyl groups themselves adopt a conformation in which the mean planes are rotated by 53.96(18)° (**2**) and 53.07(8)° (**3**).

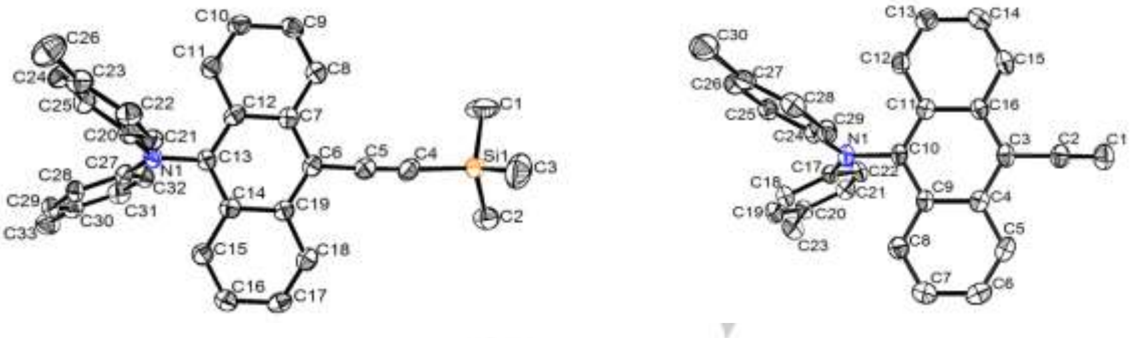

Figure 1. ORTEP. (50 % probability level) of the molecular structure of **2** (left) and **3** (right) with the atom numbering scheme. All hydrogen atoms have been omitted for clarity. Selected bond distances (Å), angles (°) and torsion angles (°) **2**: Si1–C4 1.835(6), C4–C5 1.204(8), C5–C6 1.430(8), C13–N1 1.426(7), C7–C8 1.421(8), C8–C9 1.361 (7), C7–C12 1.428(8), C9–C10 1.412(8); C6–C5–C4 178.5(6), C5–C4–Si1 177.3(5), C12–C13–N1 119.4(5), C20–N1–C27 122.4(5); C12–C13–N1–C20 -66.6(7), C28–C27–N1–C20 -27.8(7). **3**: C1–C2 1.177(3), C2–C3 1.442(3), C10–N1 1.433(2), C4–C5 1.426(3), C5–C6 1.357 (3), C4–C9 1.429(3), C6–C7 1.408(3); C1–C2–C3 178.0(3), C9–C10–N1 118.64(19), C17–N1–C24 123.66(17); C9–C10–N1–C24 -72.2(3), C18–C17–N1–C24 -34.1(3).

The electrochemical behavior of compound 4 was investigated by cyclic voltammetry using an anhydrous dichloromethane solution of $[NnBu_4][B(C_6F_5)_4]$[17] (0.1 mol·L^{-1}) as supporting electrolyte at 25 °C (see Figure 2). Since compound 4 exhibits three redox active functionalities, for comparison anthracene as well as compound 2 (bearing the triarylamino and anthracene moiety) have been measured under the same conditions. The results at 100 mV/s sweep rates are summarized in Table 1 (additional information on the reversibility can be found in the supporting information, see Figure SI3).

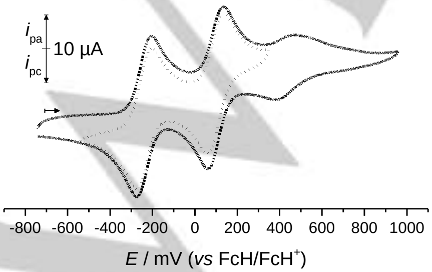

Figure 2. Cyclic voltammogram of **4** in dichloromethane using $[NnBu_4][B(C_6F_5)_4]$ (0.1 mol·L^{-1}) as supporting electrolyte *vs* ferrocene/ferrocenium. Potential range -750 mV – 1000 mV (black), -550 – 350 mV (dotted).

For compound **4** three individual redox processes can be observed of which the first two are reversible one-electron events, while the 3*rd* process appears to be irreversible. Comparison with literature known values for the Ru-half-sandwich moiety (typically -5 – -595 mV)[10,18] revealed that the 1*st* redox event is most likely the oxidation of Ru^{2+} to Ru^{3+} while subsequently the triarylamine functionality[19–21] is oxidized. However, it is noticeable that the amine oxidation occurs at a much lower potential than in compound **2**. Moreover the 3*rd* irreversible process, associated with an oxidation process at the anthracene core, is shifted about 350 mV cathodically compared to unsubstituted anthracene, despite the fact that $\mathbf{4}^{2+}$ already carries two positive charges which should result in an anodic shift of the process. This behavior may be caused by a delocalization of the electron density and hence the electron removal of delocalized π-orbitals involving all three functional groups resulting in a better stabilization of the positive charges.

Table 1. Cyclic voltammetry data of **4**, anthracene and **2**.[a]

Compound	$E_1^{\circ\prime}$ / mV[b] (ΔE_p / mV)[c]	$E_2^{\circ\prime}$ / mV[b] (ΔE_p / mV)[c]	$E_3^{\circ\prime}$ / mV[b] (ΔE_p / mV)[c]
4	-235 (61)	95 (74)	470 (101)[d]
Anthracene	815 (72)	-	-
2	355 (84)	1030[d]	-

[a] Potentials versus FcH/FcH$^+$[22–24] (scan rate 100 mV s^{-1}) at a glassy-carbon electrode of 1.0 mmol L^{-1} solutions of the analytes in dichloromethane that contained 0.1 mmol L^{-1} of [N*n*Bu$_4$] [B(C$_6$F$_5$)$_4$] as supporting electrolyte at 25 °C. [b] $E^{\circ\prime}$ = formal potential. [c] ΔE_p = difference between the cathodic and anodic peak potentials $|E_{pc} - E_{pa}|$ [d] E_{pa} irreversible process.

To further investigate the redox behavior of **4** spectroelecto UV/Vis-NIR measurements have been carried out within an OTTLE[25] (optically transparent thin-layer electrochemical) cell, using dichloromethane solutions of the analyte (2.0 mmol·L^{-1}) containing [N*n*Bu$_4$][B(C$_6$F$_5$)$_4$] (0.1 mol·L^{-1}) as supporting electrolyte.[25,26] During the measurements, the applied cell potential was increased stepwise (step width: 15 mV, 50 mV or 100 mV). The potential depending UV/Vis-NIR spectra are depicted in Figure 3 and the band characteristics are summarized in Table 2. The potential increase from -100 to 265 mV *vs* Ag/AgCl[27] resulted in the mono-oxidation of **4**. From the electrochemical investigations it is concluded that the 1*st* oxidation process is mainly located at the ruthenium redox center, however a partial delocalization with the anthracene π-system seems plausible. Therefore, an electron transfer interaction between the amine nitrogen and the ruthenium moiety *via* the anthracene backbone is expected in the low energy region of the spectra of **4$^+$**.

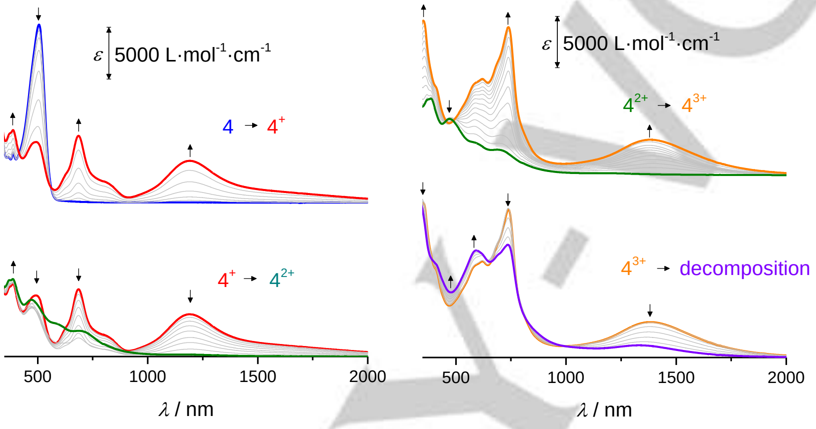

Figure 3. Spectroelectrochemical measurements of **4** within an OTTLE cell at 25 °C in dichloromethane (2.0 mmol·L^{-1}) at rising potentials (Left bottom: -100 – 265 mV; left top: 265 to 700 mV; right bottom 700 – 1050 mV; right top 1050 – 1300 mV *vs* Ag/AgCl); supporting electrolyte 0.1 mmol·L^{-1} [N*n*Bu$_4$][B(C$_6$F$_5$)$_4$]; arrows indicate rising or decreasing intensities.

Table 2. UV-Vis/NIR measurements of **4**, **4$^+$**, **4^{2+}** and **4^{3+}**.[a]

Compd. / oxidation state	origin of transition	λ / nm (ϵ_{max} / L·mol·cm^{-1})
4	π-π* (with charge transfer component from the tolylamine to anthracene)[11,14,28]	505 (17400)
4$^+$	π-π*[10,11,28]	685 (6600)
	CT-transition (involving the anthracene π system)	1195 (4150)
4^{2+}	LMCT	385 (7580)
4^{3+}	LMCT	350 (15200)
	π-π*[10,11,28]	740 (14600)
	CT-transition (involving the anthracene π system)	1380 (3500)

[a] In dichloromethane containing 0.1 mol L^{-1} of [N*n*Bu$_4$][B(C$_6$F$_5$)$_4$] as supporting electrolyte at 25 °C.

Within the spectra an absorption band at 1195 nm could be observed, which is a typical range for charge transfer excitations. Compared to other IVCT bands in unsymmetrical mixed valent systems[19,28–32] and ruthenium/iron half-sandwich aryl alkynes[10,31,33] the observed intensity of the charge transfer excitation is rather high (4150 L·mol^{-1}·cm^{-1}) with a small FWHM (full width at half maximum, $\Delta\tilde{\nu}_{½}$) of 2090 cm^{-1} which hints at a considerable degree of delocalization.[15,34–37] The IVCT band of **4$^+$** is red-shifted compared to related (symmetrical) bi- and trinuclear complexes and shows lower intensities.[11,20,38–41] Increasing the applied potential up to 700 mV resulted in the formation of **4^{2+}**. During this process the NIR absorption disappeared, which also confirms the characteristic of former band as a Ru/N charge transfer absorption. Interestingly upon the 3*rd* oxidation process a new NIR absorption is observed which resembles the one found in **4$^+$**, is however shifted towards lower energy (1380 nm; **4^{3+}**) with a lower intensity (3500 L·mol^{-1}·cm^{-1}) and a higher $\Delta\tilde{\nu}_{1/2}$ value (2350 cm^{-1}). Compound **4^{3+}** was not stable under the measurement conditions and decomposed slowly over time. This decomposition process was accelerated upon further potential increase, which reaffirms the findings during the cyclic voltammetry experiments and comparable ruthenium aryl alkynes.[10,35] Within the spectroelectro-NIR measurements the decomposition was accompanied with a decrease of the intensity of the charge transfer excitation at 1380 nm over time.

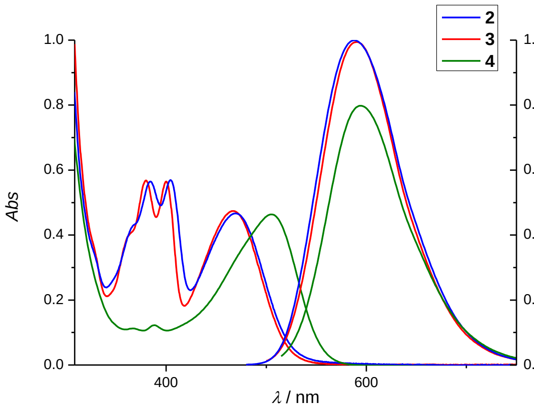

Figure 4. UV-Vis absorption (left) and fluorescence spectra (right) of **2** (blue), **3** (red) and **4** (green) in dichloromethane (1.0·10^{-5} mol·L^{-1}).

The optical properties of compounds **2**, **3** and **4** were studied by UV-vis and fluorescence spectroscopy. Figure 4 shows the absorption and emission spectra of the three substances in CH_2Cl_2. Absorption peaks of the solutions were observed at 385, 405 and 470 nm (**2**) and 380, 400 and 465 nm (**3**), as well as 500 nm (**4**) respectively. The similar absorption behavior of compounds **2** and **3** can be attributed to the electronically neutral protective trimethylsilyl group which doesn't change the absorption properties of **2** compared to the unprotected molecule **3**. Furthermore, the fluorescence spectra of **2** (585 nm), **3** (590 nm) and **4** (595 nm) showed a similar emission behavior in regard to the emission wavelength and display a bathochromic shift compared to **1** (535 nm)[14]. However, it is notable that compound **4** displays smaller emission intensities compared to **2** and **3** which can be attributed to the different absorption behavior of the complex below 500 nm due to possible trapping mechanisms introduced by the inclusion of the ruthenium moiety.[42] The emission of compound **1** was attributed to the relaxation of a charge-transfer between the electron-donating di(*p*-tolyl)tolylamine- and electron-accepting anthracenyl-moiety.[14] Hence, the emission properties of **2** and **3**, and subsequently, **4** are related to its di(*p*-tolyl)amine-anthracenyl unit and only a minor influence of the ruthenium moiety on the emission wavelength can be detected. A purely ligand-centered emission behavior is not completely uncommon for half-sandwich complexes and is displayed by a decrease of the quantum yield and emission intensities in the organometallic parent.[31,32,43]

Conclusions

The complex [CpRu^{II}(dppe)(taae)] (**4**) (Cp = cyclopentadiene, dppe = 1,2-bis(diphenylphosphino)ethane, taae = 10-ethynyl-*N*,*N*-di-*p*-tolylanthracen-9-amine) has been synthesized in a multistep reaction protocol involving Sonogashira *C*,*C* cross coupling reactions as well as Buchwald-Hartwig *C*,*N* couplings. The molecular structure of the intermediates *N*,*N*-di-*p*-tolyl-10-((trimethylsilyl)ethynyl)anthracen-9-amine (**2**) and 10-ethynyl-*N*,*N*-di-*p*-tolylanthracen-9-amine (**3**) has been determined by single crystal x-ray diffraction, revealing a bend structure of the anthracene unit. Electrochemical measurements showed that compound **4** undergoes three consecutive oxidation processes (-235 mV, 95 mV and 470 mV) whereas **4**$^{3+}$ is not very stable and decomposes. The 2*nd* and 3*rd* oxidation processes occur at much lower potentials than analogous compounds featuring similar functional units such as **2** (the triarylamine unit is oxidized at 355 mV) and anthracene (815 mV) which were measured under the same conditions. This cathodic potential shift hints to a delocalization of the electron density and thus three fold oxidation of a delocalized π orbital involving all three redox active units. This was supported by spectroelectrochemical UV/Vis-NIR measurements which demonstrated charge transfer excitations within this π system for **4**$^{+}$ and **4**$^{3+}$. Fluorescence spectroscopy of **4** on the other hand only showed a negligible influence of the ruthenium moiety on the emission wavelength and decreased emission intensities.

Acknowledgements

E. K. thanks the Saxon State Ministry for Science and the Arts for a Landesgraduierten fellowship. M. K. likes to thank the Fonds der Chemischen Industrie for their generous financial support. We are very grateful to Prof. Heinrich Lang for the supply of laboratory space and equipment. We also wish to thank Tatiana A. Shumilova and Prof. Evgeny A. Kataev for their help with the recording of the fluorescence spectra and Prof. Stefan Spange for providing access to his luminescence spectrometer.

Keywords: alkynyl complexes • electrochemistry • charge transfer • NIR-spectroelectrochemistry • ruthenium

[1] A. Burke, L. Schmidt-Mende, S. Ito, M. Grätzel, *Chem. Commun.* **2007**, 234–236.
[2] Y. Ozaki, W. F. McClure, A. A. Christy, *Near-Infrared Spectroscopy in Food Science and Technology*, Wiley-VCH Verlag GmbH, Weinheim, Germany, **2006**.
[3] C. K. Kao, *Optical Fibre Systems: Technology, Design and Application*, McGraw-Hill, USA, **1982**.
[4] M. R. Detty, S. L. Gibson, S. J. Wagner, *J. Med. Chem.* **2004**, *47*, 3897–3915.
[5] W. Kaim, *Coord. Chem. Rev.* **2011**, *255*, 2503–2513.
[6] C. Lambert, G. Nöll, *J. Am. Chem. Soc.* **1999**, *121*, 8434–8442.
[7] A. Heckmann, C. Lambert, *Angew. Chemie* **2012**, *124*, 334–404.
[8] S. Dapperheld, E. Steckhan, K. G. Brinkhaus, T. Esch, *Chem. Ber.* **1991**, *124*, 2557–2567.
[9] A. P. Shaw, J. R. Norton, D. Buccella, L. A. Sites, S. S. Kleinbach, D. A. Jarem, K. M. Bocage, C. Nataro, *Organometallics* **2009**, *28*, 3804–3814.
[10] M. A. Fox, R. L. Roberts, W. M. Khairul, F. Hartl, P. J. Low, *J. Organomet. Chem.* **2007**, *692*, 3277–3290.
[11] W. Polit, T. Exner, E. Wuttke, R. F. Winter, *Bioinorg. React. Mech.* **2012**, *8*, 85–105.
[12] J. F. Hartwig, *Acc. Chem. Res.* **1998**, *31*, 852–860.
[13] X. Liu, J. Zhu, *J. Phys. Chem. B* **2009**, *113*, 8214–8217.
[14] P. Rajamalli, P. Gandeepan, M.-J. Huang, C.-H. Cheng, *J. Mater. Chem. C* **2015**, *3*, 3329–3335.
[15] U. Pfaff, A. Hildebrandt, M. Korb, S. Oßwald, M. Linseis, K. Schreiter, S. Spange, R. F. Winter, H. Lang, *Chem. - A Eur. J.* **2016**, *22*, 783–801.
[16] K. Sonogashira, Y. Tohda, N. Hagihara, *Tetrahedron Lett.* **1975**, *16*, 4467–4470.
[17] R. J. LeSuer, C. Buttolph, W. E. Geiger, *Anal. Chem.* **2004**, *76*, 6395–6401.

[18] U. Pfaff, A. Hildebrandt, M. Korb, D. Schaarschmidt, M. Rosenkranz, A. Popov, H. Lang, *Organometallics* **2015**, *34*, 2826–2840.

[19] G. Grelaud, M. P. Cifuentes, T. Schwich, G. Argouarch, S. Petrie, R. Stranger, F. Paul, M. G. Humphrey, *Eur. J. Inorg. Chem.* **2012**, *2012*, 65–75.

[20] K. Onitsuka, N. Ohara, F. Takei, S. Takahashi, *Dalton Trans.* **2006**, *2*, 3693–3698.

[21] A. Ruff, E. Heyer, T. Roland, S. Haacke, R. Ziessel, S. Ludwigs, *Electrochim. Acta* **2015**, *173*, 847–859.

[22] J. R. Aranzaes, M.-C. Daniel, D. Astruc, *Can. J. Chem.* **2006**, *84*, 288–299.

[23] I. Noviandri, K. N. Brown, D. S. Fleming, P. T. Gulyas, P. A. Lay, A. F. Masters, L. Phillips, *J. Phys. Chem. B* **1999**, *103*, 6713–6722.

[24] G. Gritzner, J. Kuta, *Pure Appl. Chem.* **1984**, *56*, 461–466.

[25] M. Krejčik, M. Daněk, F. Hartl, *J. Electroanal. Chem. Interfacial Electrochem.* **1991**, *317*, 179–187.

[26] A. Hildebrandt, H. Lang, *Organometallics* **2013**, *32*, 5640–5653.

[27] Please, note that under our conditions ferrocene is oxidized at ca. 475 mV *vs* Ag/AgCl within the OTTLE cell, however the electrode set up in this thin layer cell does not allow for accurate electrochemical measurements.

[28] W. Polit, P. Mücke, E. Wuttke, T. Exner, R. F. Winter, *Organometallics* **2013**, *32*, 5461–5472.

[29] R. C. Rocha, H. E. Toma, *Inorganica Chim. Acta* **2000**, *310*, 65–80.

[30] S.-H. Wu, J.-Y. Shao, H.-W. Kang, J. Yao, Y.-W. Zhong, *Chem. - An Asian J.* **2013**, *8*, 2843–2850.

[31] F. de Montigny, G. Argouarch, T. Roisnel, L. Toupet, C. Lapinte, S. C.-F. Lam, C.-H. Tao, V. W.-W. Yam, *Organometallics* **2008**, *27*, 1912–1923.

[32] K. M.-C. Wong, S. C.-F. Lam, C.-C. Ko, N. Zhu, S. Roué, C. Lapinte, S. Fathallah, K. Costuas, S. Kahlal, J.-F. Halet, *Inorg. Chem.* **2003**, *42*, 7086–7097.

[33] N. Gauthier, N. Tchouar, F. Justaud, G. Argouarch, M. P. Cifuentes, L. Toupet, D. Touchard, J.-F. Halet, S. Rigaut, M. G. Humphrey, et al., *Organometallics* **2009**, *28*, 2253–2266.

[34] K. D. Demadis, C. M. Hartshorn, T. J. Meyer, *Chem. Rev.* **2001**, *101*, 2655–2686.

[35] F. Paul, B. G. Ellis, M. I. Bruce, L. Toupet, T. Roisnel, K. Costuas, J.-F. Halet, C. Lapinte, *Organometallics* **2006**, *25*, 649–665.

[36] C. Creutz, in *Prog. Inorg. Chem.*, John Wiley & Sons, Inc., **1983**, pp. 1–73.

[37] N. S. Hush, in *Prog. Inorg. Chem.*, John Wiley & Sons, Inc., **1967**, pp. 391–444.

[38] G. Grelaud, O. Cador, T. Roisnel, G. Argouarch, M. P. Cifuentes, M. G. Humphrey, F. Paul, *Organometallics* **2012**, *31*, 1635–1642.

[39] M. A. Fox, B. Le Guennic, R. L. Roberts, D. A. Brue, D. S. Yufit, J. A. K. Howard, G. Manca, J.-F. Halet, F. Hartl, P. J. Low, *J. Am. Chem. Soc.* **2011**, *133*, 18433–18446.

[40] J. Chen, R. F. Winter, *Chem. - A Eur. J.* **2012**, *18*, 10733–10741.

[41] N. Gauthier, G. Argouarch, F. Paul, L. Toupet, A. Ladjarafi, K. Costuas, J.-F. Halet, M. Samoc, M. P. Cifuentes, T. C. Corkery, et al., *Chem. - A Eur. J.* **2011**, *17*, 5561–5577.

[42] F. Malvolti, C. Rouxel, G. Grelaud, L. Toupet, T. Roisnel, A. Barlow, X. Yang, G. Wang, F. I. Abdul Razak, R. Stranger, et al., *Eur. J. Inorg. Chem.* **2016**, *2016*, 3868–3882.

[43] R. J. Lavallee, C. Kutal, *J. Organomet. Chem.* **1998**, *562*, 97–104.